ELSEVIER

Chemical Engineering Journal 73 (1999) 191–204

Chemical Engineering Journal

Weir flow and liquid height on sieve and valve trays

E.F. Wijn[*,1]

Meteorenweg 1014, 1443 BD Purmerend, The Netherlands

Received 13 August 1998; accepted 11 November 1998

Abstract

Mechanisms for the flow of liquid over outlet weirs of distillation and absorption trays are described in this paper. Weir flow contributes to the liquid height on a tray, and this height is important for the design and operation of trayed columns. Comparisons of available experimental data with Francis' weir equation and with new stochastic liquid flow models showed that the traditionally used Francis' equation needs modification. The stochastic flow models link the weir flow to the flow mechanisms upstream of the tray outlet. These upstream mechanisms provide the input needed for a new weir crest equation. The existence of a so-called 'edge-vortex' (a horizontal roll cell at the boundary of the gassed and the ungassed region) is shown to play an important role, when a calming zone is present upstream of the outlet weir.

Keywords: Absorption; Calming zone; Distillation; Liquid height; Regime; Sieve tray; Spray; Valve tray; Weir

1. Introduction

Understanding the hydrodynamics controlling the liquid height on trays is central to the design and operation of distillation and absorption columns. It has an influence on the pressure drop, tray efficiency, upper and lower operating limits and flow regime on a tray. The study of the underlying flow mechanisms is of direct practical importance. Potentially, for existing columns, it may lead to raised column throughputs and/or to an improved quality of operation. Also, it may lead to improved design methods for new columns. The liquid height depends on the gas and liquid loads, gas and liquid properties and a number of geometrical parameters, such as weir height and length, free hole area, hole diameter, etc. Existing relations for the liquid height are empirical and not completely satisfactory.

In this paper, we attempt to improve upon the usual approach by proposing a more realistic description for liquid flowing over an outlet weir. This description connects the mechanisms of liquid flow across the contacting area of a tray to those over the outlet weir. It is applied to trays operating in the 'spray' regime as well as in the 'heterogeneous bubbling' regime.

2. Flow regimes

Usually, the two-phase dispersion in the contacting area of a tray is either in the *spray* or the *heterogeneous bubbling* regime, which is also known as the *churn turbulent* regime or (mixed) froth regime. Operation in the spray regime is associated with low liquid rates, low liquid heights and high gas rates. Conversely, the heterogeneous bubbling regime is favoured by high liquid rates, high liquid heights and low gas rates. In the spray regime, the gas phase is the continuous phase and the liquid phase is being atomised near the tray holes. In the contacting area, droplets move around in a random ballistic fashion. The droplet population has a wide size and velocity distribution. In the heterogeneous bubbling regime, the two-phase layer consists of at least two layers: a high-density bottom layer and a low-density top layer of spray, with a transition from liquid-continuous to gas-continuous in between. Often a relatively gas-free layer is situated directly above the floor next to the holes. Invariably, the top layer consists of a low-density spray layer, whose droplets move around in a random ballistic fashion. The heights of the separate layers contributing to the overall dispersion height vary considerably, depending on the operating conditions, system properties, tray type and tray geometry.

Nowadays, most trays operate in or close to the 'heterogeneous bubbling' regime. In this regime, the two-phase mixture has a liquid volume fraction ε_L varying in the range

*E-mail: wijnef@euronet.nl

[1]Formerly at Shell Research, Amsterdam, The Netherlands. Internet homepage URL: http://www.euronet.nl/~wijnef

1385-8947/99/$ – see front matter
PII: S1385-8947(99)00045-5

from about 0.2 to 0.6. The bed height, density and pressure drop fluctuate wildly. At the same time, there is much coalescence and break up of bubbles and drops. Together, these processes lead to a dynamic equilibrium in bubble size with a wide distribution, ranging from small 'ionic' bubbles of less than 0.5 mm to large bubbles ('voids') greater than 25 mm and having a wide bubble rise velocity distribution. The major part (or even all) of the gas flow will be transported by the large bubble ('void') phase. The liquid phase can be approximated by a 'heavy' phase, defined as an 'aerated' continuous liquid phase (including any small bubbles moving along with it), with an effective density of $\varepsilon_{L,df}\rho_L$. Random movements in the continuous phase feed back into the bubble formation process, causing desynchronization of bubble formation at adjacent orifices randomizing the initial size and the formation frequency. Because the flow on a tray is so complicated, most of the current descriptions are purely empirical. We can only begin to describe what is going on in terms of 'averaged properties'.

3. Liquid height and liquid transport

The amount of liquid on a tray is closely related to the flow regime. There are three common ways of describing the liquid height.

1. The early method of correlating the liquid height on a tray was inherited from earlier work on bubble cap trays, and assumed the liquid height to be a linear function of the weir height, gas load (F factor) and liquid load

$$H_L = \alpha H_w + \beta F + \gamma L + \delta \quad (1)$$

   A large number of references use this method. These will be discussed later.
2. A later empirical method, used among others by Hofhuis and Zuiderweg [1], employs a power law function

$$H_L = \text{constant}\, H_w^p (Q_L/L_w)^q \lambda^r f_h^s d_h^t \quad (2)$$

   It includes the effects of weir height, liquid load per unit weir length, gas load (λ factor), fractional free hole area and hole diameter. This method is not discussed further here.
3. A third, more fundamental, method, considers the liquid height to consist of two parts: one below and one above the weir

$$H_L = \varepsilon_{L,uw} H_w + H_{ow} \quad (3)$$

This method has been revised and updated by Bennett et al. [2], Colwell [3], Solomakha et al. [4,5] and Stichlmair [6]. Stichlmair also added a third term, Δ_H, to account for the liquid content in the spray layer ($\Delta_H = \varepsilon_L \Delta H_B$) by

$$\Delta_H = 125\varepsilon_L \rho_g (U_g - U_b)^2 / g(\rho_L - \rho_g)^2 (1 - \varepsilon_L)^2 \quad (4)$$

Using $Q_L = u_{L,ow} L_w H_{ow}$, Eq. (3) becomes

$$H_L = \varepsilon_{L,uw} H_w + (Q_L/L_w)/u_{L,ow} \quad (5)$$

Eq. (5) requires a knowledge of the average liquid volume fraction below the weir level ($\varepsilon_{L,uw}$) as well as on the average liquid flow velocity over the outlet weir ($u_{L,ow}$). Under the influence of gravity, the average liquid volume fraction below the weir ($\varepsilon_{L,uw}$) is larger than the average liquid volume fraction of the entire dispersion (ε_L). An empirical equation from Solomakha et al. [4] gives this ratio as $\varepsilon_{L,uw}/\varepsilon_L = (0.38 + L_{cz})/\sqrt{H_w}$. Here, L_{cz} is the distance between the perforations and the outlet weir.

Three mechanisms for the transport of liquid over a weir will be considered to obtain the flow velocity ($u_{L,ow}$)

1. the classical mechanism of clear liquid flow over a weir, leading to Francis formula;
2. stochastic splashing of drops over a weir, in the spray regime;
3. stochastic displacement of 'packets' of liquid over a weir, in the heterogeneous bubbling regime.

3.1. Francis' weir equation

The height required by clear liquid flowing over a weir is given by $H_{ow} = 1.43[(Q_L/L_w)^2/g]^{1/3}$. For a dispersion, the clear liquid height H_{ow} has to be replaced by the dispersion height and the liquid flow Q_L by the dispersion flow. Assuming that, in a two-phase dispersion the continuous phase is homogeneous, this can be transformed by use of the liquid volume fraction in the dispersion $\varepsilon_{L,ow}$ into $H_{ow}/\varepsilon_{L,ow} = 1.43[\{(Q_L/\varepsilon_{L,ow})/L_w\}^2/g]^{1/3}$. Here $H_{ow}/\varepsilon_{L,ow}$ is the dispersion height above the weir and $Q_L/\varepsilon_{L,ow}$ is the volume flow of the 'aerated' liquid over the weir. Rearrangement gives

$$H_{ow} = 1.43[\varepsilon_{L,ow}(Q_L/L_w)^2/g]^{1/3} \quad (6)$$

This equation results in $u_{L,ow} = [g(Q_L/L_w)/\varepsilon_{L,ow}]^{1/3}/1.43$ for the average weir flow velocity. With $\varepsilon_{L,ow} = 1.00$ and $0.001 < Q_L/L_w < 0.01\ \text{m}^3\ \text{s}^{-1}\ \text{m}^{-1}$, these weir flow velocities are in the range of $0.15 < u_{L,ow} < 0.30\ \text{ms}^{-1}$.

This model assumes streamline gravitational flow of a clear liquid over the outlet weir. It does not take into account the high degree of random motion in the two-phase mixture.

3.2. Splashing of droplets

At low liquid rates, low liquid heights and high gas rates, the dispersion on a tray will be a spray. The drops are moving randomly in every horizontal direction, while executing their vertical ballistic trajectories. As a group, they have a *horizontal* velocity distribution (Fig. 1). As we shall see, the spread in the horizontal droplet velocity is much higher than the mean horizontal liquid flow velocity,

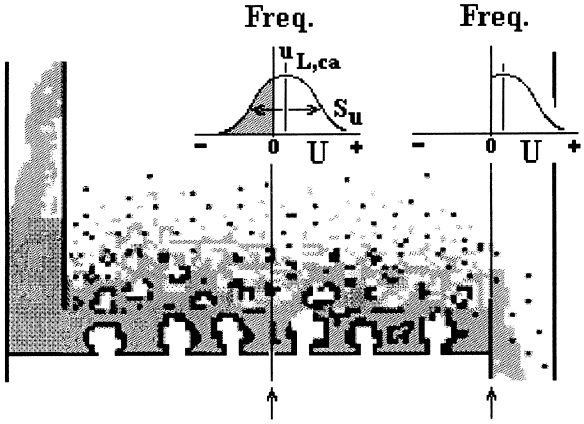

Fig. 1. Horizontal velocity distributions.

$u_{L,ca}(= Q_L/(W_{ca}H_L))$. As no further preferential flow direction is imposed, the distribution of velocities in the middle of the contacting area will be assumed to be symmetric. Above the weir, all drops move away from the contacting area into the downcomer; these are the drops from the right half of the centre distribution. So, at the weir, the flow rate of suspended drops will be one-half of that in the centre of the tray. Consequently, the liquid height over the weir (the weir crest) will be one-half of the liquid height in the centre of the tray: $H_{ow} = (1/2)H_{ow,ca}$. The average velocity of the drops flowing over the weir can now be equated to the variance of the horizontal velocity distribution: $u_{L,ow} = S_U$.

This stochastic transport of drops can be likened to the behaviour of particles on a 'vibrating conveyer' (with one-directional motion) or a 'vibrating screener' (with two-directional horizontal motion).

An important condition for this mechanism to work is that the liquid has to be suspended in order to be transported over the weir. The liquid has to be kept in this 'suspended' state by the gas passing upward through the dispersion, transferring its kinetic energy to the drops and driving an upward moving (and subsequently downfalling) liquid flux Q_o/A_{ca}. The amount of liquid in the suspended drop layer is obtained by multiplication of this flux with the time of flight: $h_{L,spray} = tQ_o/A_{ca}$. (Note that this is Stichlmair's Δ_H.) Thus the suspended hold-up of liquid should be sufficient to provide the required weir crest $h_{L,spray} \geq H_{ow,ca}$.

There are several references allowing an estimate of the *vertical* drop velocities. From the droplet projection velocity data of Aiba and Yamada [7] and Pinczewski and Fell [8], it can be seen that, for sieve trays, these fall in the range of $U_o \approx 1$–$2\ \mathrm{ms}^{-1}$, and have a standard deviation of approximately 0.1–0.2 for drops sufficiently large to be unaffected by gas drag. From Stichlmair's equation [6] for the liquid height in the spray layer on sieve trays, a relation for the droplet projection velocity U_o can be recovered (used later in this paper): $U_o = 11.2\lambda_{ca}(1 - U_b/U_g)/(1 - \varepsilon_L) \cong 11.2\lambda_{ca}$. The projection velocity is proportional to the gas load factor and includes corrections for the bubble rise velocity U_b and liquid volume fraction ε_L. Bennett and Grimm [9] give another similar relation, which can be written as

$$U_o = \lambda_{ca}\sqrt{[9\sqrt{3}/(f_h\varepsilon_L)]}$$

Their equation also proposes a linear relation between the projection velocity and gas load factor, but a different effect of liquid volume fraction and includes an effect of the hole free area. However, both relations produce approximately the same values for the projection velocity, U_o.

Drops will be projected upward over a height: $\Delta H = U_o^2/2g$=0.05–0.20 m. This is sufficient to let them jump over the weir. The time that a drop is suspended (its time of flight) is $t = 2U_o/g$=0.2–0.4 s. The horizontal component of the drop velocity is expected to be considerably less than the vertical velocity: $u_{L,hor} = 0.1$–$0.2\ U_o = 0.1$–$0.4\ \mathrm{ms}^{-1}$. This means that drops may be expected to travel horizontally over a distance scale of $L_{hor} = u_{L,hor}t$ =0.02–0.16 m. Only droplets generated within this distance L_{hor} from the weir will be able to jump out of the contacting area and leave the tray. The velocities of the leaving droplets are typically in the range of $0.1 < u_{L,ow} < 0.4\ \mathrm{ms}^{-1}$.

3.3. Splashing of 'packets' of liquid by large bubbles

In the heterogeneous bubbling regime, the phases are reversed and the mechanism 'driving' the stochastic horizontal motion is different. Ashley and Haselden [10] have shown that gas passes upward through the liquid phase mainly as large bubbles ('voids'). Bubble rise velocities on sieve trays have been reported by Raper et al. [11]. For bubble sizes ranging from 20 to 80 mm, they found rise velocities in the range of $0.6 < U_b < 1.2\ \mathrm{ms}^{-1}$. Ellenberger [12] and de Swart [13], working with bubble columns and fluidized beds, found $0.4 < U_b < 1.1\ \mathrm{ms}^{-1}$ for large bubbles with diameters from 20 to 120 mm.

Because of these large escaping bubbles ('voids'), the upper surface of the gas–liquid mixture fluctuates wildly. These large bubbles displace (at least) their own volume of liquid in all directions. One-half of this liquid volume is displaced in the direction of the tray outlet and can splash over the weir. The scale and velocity of the displacement are near the size and rise velocity of the large bubbles, possibly a little lower, in the range of $0.5 < u_{L,ow} < 1.0\ \mathrm{ms}^{-1}$.

Note that the three mechanisms can produce similar weir flow velocities. This allows the following statements to be made. A specified liquid flow rate can be transported over an outlet weir, by random motion, at similar weir crest heights as for the idealized case of a free falling flow of liquid over a weir (Francis' case). Secondly, considerable deviations from Francis' weir equation should be expected, depending on the flow regime, gas/liquid properties, operating conditions, tray geometry, etc.

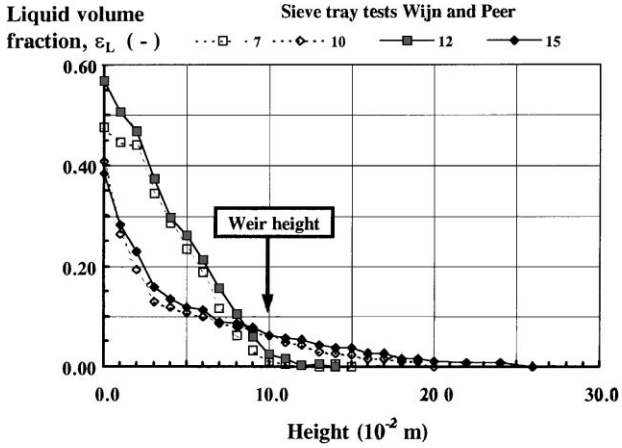

Fig. 2. Some liquid volume fraction profiles.

4. Measurements on tray liquid

Experimental profiles of the vertical distribution of the liquid on a tray can yield the liquid height, the dispersion height and the average liquid volume fraction. Also, they allow the flow regime to be recognized as well as possible stratification in the two-phase layer. Several techniques have been used to obtain density profiles. Solomakha et al. [4] used an electric capacitance technique. Hofhuis and Zuiderweg [1,14,15] and Pinczewski and Fell [16], as well as the author, used λ ray attenuation. Integration of experimental profiles of the liquid volume fraction is the most direct way to find the amount of liquid above the outlet weir, the weir crest H_{ow}. Preferably, this should be done as close to the weir as possible. Usually, however, these profiles are obtained near the centre of the tray. So they represent the two-phase behaviour in the contacting area.

Fig. 2 shows examples of the density profiles acquired by the author in the central area of a rectangular air–water simulator (see Fig. 4 for the operating conditions for the runs identified by the labels).

In the literature, there is not much experimental information available on density profiles. Five data sets are used here, of which four sets are for sieve trays and one is for a valve tray. One data set on five different sieve tray layouts originates from the work of Pinczewski and Fell [16]; two sets stem from the work of Hofhuis [14] and will be referred to as Hofhuis/Meijer (for data obtained in the 0.45 m diameter SRTCA test column with boiling toluene as test system) and Hofhuis/van Driesten (for data obtained in the 0.8×1.0 m Delft air–water simulator). From the work of this author at SRTCA, a data set for each of two modifications of one sieve tray layout and a data set for one valve tray layout will be presented. Relevant data on the trays used can be found in Table 1 and in the references. The scale of the test units was large enough for the hydraulic behaviour on the trays to be representative for large-scale commercial tray columns.

For the sieve trays, Fig. 3 presents the weir crest data as a function of the specific weir load Q_L/L_w. The data of Pinczewski are introduced first, because his profiles were the first profiles available and because he varied the free area of the tray. He experimented with a low weir, but at the same time applied relatively large specific weir loads, which resulted in a large contribution of the weir crest to the liquid height $H_{ow,ca}/H_L \cong 0.6$–0.8, and a relatively low liquid height on his trays. With the applied gas velocities, the two-phase layer on his trays consisted largely of droplets (with a wide size distribution and originating slightly above the tray deck) and operated predominantly in the spray regime. In Fig. 3, we see that his data aggregate along the line representing Francis' weir equation for clear liquid. The average ratio of the experimental over calculated weir crest for his data set was found to be $H_{ow,exp}/H_{ow,Fr} = 0.88 \pm 0.12$. This shows that Francis formula does a reasonable job, although the observed transport mechanism is quite different from that assumed. Notice also that a variation in free area and hole size did not influence the weir crest in the data of Pinczewski. Neither did a variation in gas load (load factor λ) have a noticeable effect.

Co-operatively, Hofhuis, Meijer and the author have done tests on a sieve tray in a 0.45 m diameter distillation column of Shell Research at Amsterdam. These tests have been presented before [1,14,15]. On these sieve trays there was no calming zone next to the outlet weir. During the tests,

Table 1
Tray geometries and test conditions

Source	Tray type	Hole diameter (mm)	Free area (%)	Weir height (m)	Calm. zone (m)	λ_h-range (ms^{-1})	H_L range (mm)	Column size (m)	Test system
Pinczewski	Sieve	6.3	11.0	0.025	0.05	0.5–1.3	14–22	0.3×0.6	air–water
Pinczewski	Sieve	12.7	5.9	0.025	0.05	0.5–1.3	14–22	0.3×0.6	air–water
Pinczewski	Sieve	12.7	10.7	0.025	0.05	0.5–1.3	14–22	0.3×0.6	air–water
Pinczewski	Sieve	12.7	16.1	0.025	0.05	0.5–1.3	14–22	0.3×0.6	air–water
Pinczewski	Sieve	19.0	10.3	0.025	0.05	0.5–1.3	14–22	0.3×0.6	air–water
Hofhuis/Meijer	Sieve	7.0	10.0	0.050	0.01	0.4–1.3	6–33	0.45 m	toluene
Hofhuis/van Driesten	Sieve	7.0	10.0	0.050	0.10	0.25–1.10	20–40	0.8×1.0	air–water
Wijn/Peer(a)	Sieve	2.5	19.4	0.100	0.01	0.20–0.55	11–28	0.3×0.6	air–water
Wijn/Peer (b)	Sieve	2.5	19.0	0.100	0.16	0.20–0.55	21–49	0.3×0.6	air–water
Wijn/Konijn	Valve	40.0	15.8	0.100	0.03	0.05–0.55	9–108	0.3×0.6	air–water

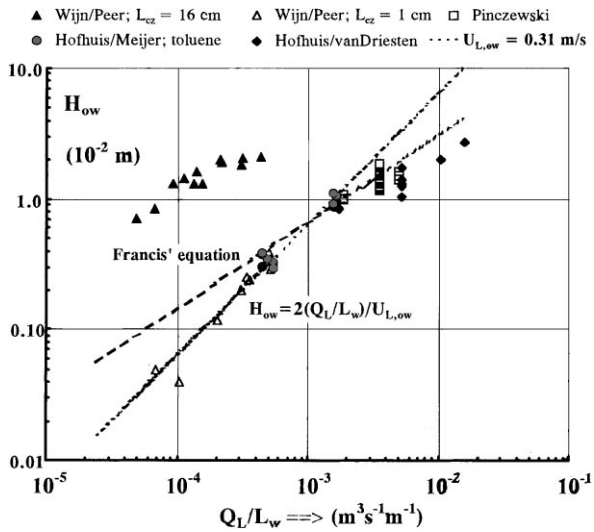

Fig. 3. Comparison of weir crest relations for sieve trays.

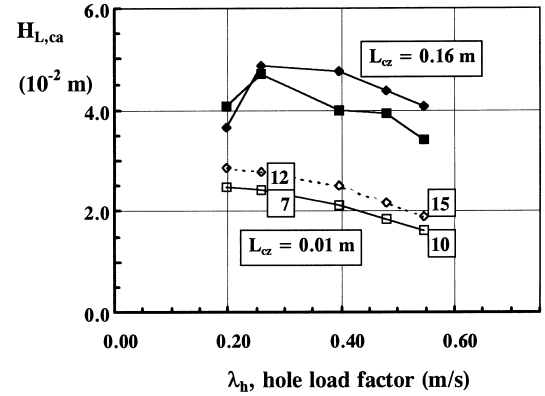

Fig. 4. Effect of calming zone on liquid height.

chemically pure toluene was 'distilled' at atmospheric pressure. At two different liquid flow rates, the vapour flow rate was varied. The test column had view ports, so the vapour/liquid behaviour on the trays could be observed. From observations, photos and density profiles (with a minimum and maximum density bulge, as in Pinczewski's profiles), it was clear that this sieve tray operated in the spray regime, with droplets being ejected from just above the tray floor. The contribution of the weir crest to the liquid height varied considerably: $H_{ow,ca}/H_L \cong 0.1–0.8$.

Wijn and Peer collected a data set which allowed several hydraulic mechanisms on a sieve tray to be elucidated. The tray had small holes was tested in two configurations: (a) with no calming zone next to the weir ($L_{cz} = 0.01$ m) and (b) with a long calming zone ($L_{cz} = 0.16$ m). The layout with the long calming section also had a 30% smaller hole area (0.0235 m^2 against 0.0340 m^2 originally). The hole free area was high and with the high weir this led to operation close to or in the weeping range. The air–water simulator had facilities to measure separately: the flow rate to the tray; the weep flow rate; and the downcomer flow rate (yielding the specific weir flow rate). The tests were run at fixed liquid feed flow rates, while the gas flow rate was varied.

The data are presented in two parts to show the large difference resulting from the introduction of the long calming zone. Weeping rates increased (indeed), pressure drops increased, liquid heights increased, the dispersion height increased and movements in the dispersion became much more pronounced (violent). Fig. 4 shows the liquid height as a function of the hole load factor λ_h. It contains data for two liquid feed flow rates. The large difference in weir crest for these two sets can be seen in Fig. 3.

Some observations on the hydraulic behaviour can be added.

For the layout without a calming zone ($L_{cz} = 0.01$ m): The operating range of the tray varied from the seal point to well above the weep point. The height of the two-phase layer ranged from about equal to the weir height to well above it. On the small ledge next to the outlet weir, the height of clear liquid was never seen to be higher than 0.04 m: this is far below the weir height and no continuous phase could be seen going over the weir. So, only droplets were jumping over as the upper spray layer was being 'sampled' by the outlet weir. As the sieve tray was weeping at the same time, this reduced the liquid flow rate coming into the downcomer and resulted in fairly low specific weir loads. The weir crest contribution to the liquid height ranged was $H_{ow,ca}/H_L \cong 0.05–0.20$.

For the layout with long L_{cz} and reduced hole area: The range of operation shifted more deeply into the weeping range because of the increased liquid height (in agreement with the weep model presented before [17]). The clear liquid height on the calming zone next to the weir rose also, but never exceeded a height of 0.07 m, still well below the weir height. So again, the weir load was caused by splashing droplets only. The low hole load factors ensured operation of the holes in the bubble formation mode. So, a heterogeneous bottom-layer was present underneath the top layer of spray. The weir crest contribution to the liquid height increased and varied between $H_{ow,ca}/H_L \cong 0.1$ and 0.8. The liquid height in the contacting area was consistently lower than the liquid height in the calming zone, at $H_L \cong 0.5–0.7\ H_{L,cz}$.

The rectangular 0.8 × 1.0 m air–water simulator at Delft Technical University was used by Hofhuis and van Driesten to obtain a collection of density profiles. The eight profiles published in the Hofhuis and Zuiderweg paper [1] are used here, as examples of their data set and as a check. Gas flow rate and weir loadings were varied over a wide range. The tray was operated in several flow regimes: the spray and the heterogeneous flow regime were both encountered. The weir crest contribution to the liquid height varied between $H_{ow,ca}/H_L \cong 0.3$ and 0.7. The authors observed that the liquid height in the contacting area was consistently lower than on the 0.10 m long calming zone: $H_L \cong 0.55–0.70\ H_{L,cz}$.

The next dataset presents test results for a different type of tray. Wijn and Konijn tested a tray provided with *Shell/*

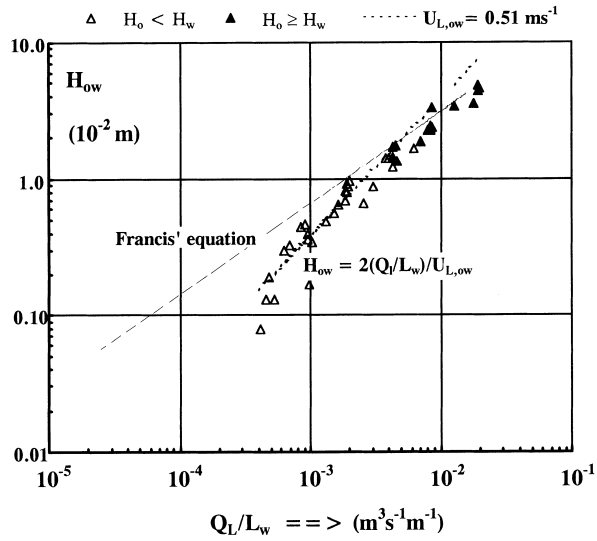

Fig. 5. Comparison of weir crest relation for a valve tray.

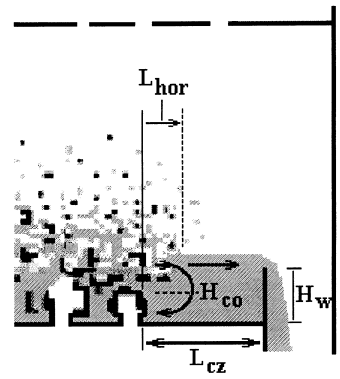

Fig. 6. Calming zone with 'edge-vortex'.

Metawa valves, in the same air–water simulator as used by Wijn and Peer. The weir crest results are presented in Fig. 5. The valve tray allowed tests to be done over a much wider range of gas flow rates and weir flow rates than for the sieve trays. The same techniques were used again. γ Ray attenuation was used to obtain the density profiles. The weir crest was obtained by integration of these profiles. The specific weir load was found from the measured downcomer liquid flow rate. The weir crest contribution to the liquid height varied between $H_{ow,ca}/H_L \cong 0.02$ and 0.65. The liquid height in the contacting area was consistently lower than the liquid height on the short 0.03 m calming zone, varying in the range $H_L \cong 0.47$–$0.92\ H_{L,cz}$.

5. The 'edge-vortex' model

A calming zone next to an outlet weir provides distance and time for droplets to fall out of the gas phase and for degassing of the liquid phase, before the liquid disappears into the downcomer entrance (Fig. 6). Up to now, there has been no consensus on whether such a calming zone has an effect on the tray upstream. The example of Wijn and Peer shows how effectively a calming zone can alter the tray hydraulics. To take this effect into account the 'edge-vortex' model has been developed. Subsequently, the model was compared with available data. Additional material on the calming zone effect can be found in Solomakha et al. [4], Huang and Hodson [18], Detman [19], Vikhman et al. [20] and Lockett [21].

The insights gained so far can be used to estimate the length scale of the zone actively contributing to the splashing weir flow. 50% of the flow over the weir originates within a distance determined by the average drop flight time and the average horizontal velocity $L_{50\%} = u_{L,ow}t$, with $t = 2\ U_o/g$. This yields in dimensionless form: $gL_{50\%}/U_o^2 = 2u_{L,ow}/U_o$. Substituting Stichlmair's sieve tray relation for U_o, it is found that $L_{50\%} \cong 22.4\lambda_{ca}u_{L,ow}/g$ and so $L_{50\%} \cong 0.67\ \lambda_{ca}$. Thus, the zone actively splashing drops over a weir grows with the gas load factor, λ_{ca}. For the typical range $0.03 < \lambda_{ca} < 0.10\ \mathrm{ms}^{-1}$, this length scale becomes $0.02 < L_{50\%} < 0.07$ m. So, a large part of the splashing weir flow rate originates close to the outlet weir. The full weir flow rate comes from a distance some 2–3 times longer, $0.06 < L_{hor} < 0.2$ m. (confirming the early estimate). On the basis of this line of reasoning, the length of the calming zone in the experiment of Wijn and Peer was chosen as $L_{cz} = 0.15$ m. In this respect, the 0.10 m long calming zone used in the experiments of Hofhuis and van Driesten [14,33] was long enough to have had an effect on (at least a part of) their results.

At the *boundary* of the contacting area and any unperforated edges around it, there is a large contrast in clear liquid height and bed height. At these edges, a liquid recycle (vortex) is present, which is driven by the difference in static pressure on each side. This pressure difference is maintained by the gas flow through the contacting area, which expands ('pumps up') the liquid phase to a height exceeding the weir level. Furthermore, the pressure difference will be augmented by the pressure reducing ('sucking') effect of the high velocity gas jets issuing from the holes in the tray floor.

A simple '*edge-vortex*' model has been developed to clarify the relation between the two liquid heights, the bed expansion and the recycle flow rate. The recycle flow rate can be compared to the specific weir flow rate to show its importance. Assume the liquid phase to be an essentially gas-free liquid phase (not aerated). Then, the liquid height on the calming zone is governed by the flow of clear liquid over the outlet weir, and Francis' equation can be used; $H_{L,cz} = H_w + H_{ow,Fr}$. Also, assume that the two-phase layer in the contacting area has a uniform density distribution along the height (constant liquid volume fraction). This is an oversimplification, but going into more detail in describing the porosity profile in the contacting area is beyond the scope of this paper. These assumptions lead to linear static pressure gradients on the calming zone and contacting area

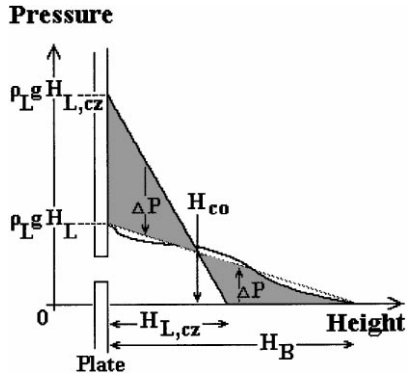

Fig. 7. Pressure gradients.

as depicted in Fig. 7. Then the height at which these gradients cross each other is located at

$$H_{co}/H_{L,cz} = [1 - (H_L/H_{L,cz})]/(1 - \varepsilon_L).$$

The difference in pressure between the calming zone and contacting area drives a flow of liquid between them. The pressure difference used in Bernoulli's equation gives an estimate for the local liquid velocity of $u = \sqrt{(2\Delta P/\rho_L)}$. Then, the local liquid velocity will be a function of height above the tray floor, as can be deduced from Fig. 7. There are three ranges in height to consider

1. $h \leq H_{co}$, near the plate floor, liquid flows back from the calming zone into the contacting area (note that the back flowing bottom layer can be considered to act like a 'dynamic and open weir' because the outflow from the contacting area has to flow over it, onto the calming zone);
2. $H_{co} < h < H_{L,cz}$, liquid flows to the weir with a velocity increasing from zero to a maximum at $H_{L,cz}$;
3. $H_{L,cz} < h < H_B$, again to the weir with a velocity decreasing from a maximum at $H_{L,cz}$ to zero at H_B.

The total liquid flow rate across the boundary is found by integration of the velocity profile over the full dispersion height.

Consider the dispersion height and the liquid height on the calming zone as given. Further, require that the ratio of the liquid outflow and backflow has a specific value, $R = (Q_L + Q_{L,back})/Q_{L,back}$. Also, choose a liquid volume fraction for the expansion of the bed in the contacting area. Then, the problem is sufficiently specified and can be solved for the liquid height and the actual flow rate of the recycle.

The ratio R depends on the geometry of the tray. Important points are whether the non-perforated zone is located: next to the column wall; as 'blanking' strips in the contacting area; on the inlet side of the tray; or near the outlet weir.

In the first two cases, there is no net liquid flow in or out and $R = 1$. In the other two cases, there is either a net liquid flow in or a net flow out, and this is equal to the liquid feed flow rate to the tray (with $R \leq 1$ at the inlet and $R \geq 1$ near the outlet).

The desired relationship between the recycle flow rate, bed expansion (characterised by ε_L) and liquid height in the contacting area can be derived in the following way. Assign a value to the flow ratio R characterizing the recycle and start off by using $dQ_L = \varepsilon_L u_L W dh$. Then relate the local velocity u to the local pressure difference obtained from the two liquid height gradients. Also, note that the area available to the liquid backflow through the boundary is only partly open to the flow of liquid because upflowing gas is blocking part of it. Next, the liquid backflow is found by integration from the tray floor up to the height H_{co}, where the pressure gradients cross. Finally, the outflow can be found by integrating further up to the bed height and should be equal to $RQ_{L,back}$. Remember that usually the backflow $Q_{L,back} >> Q_L$ (especially when operating at low liquid rates in the spray regime). Normally, it is to be expected that $R \geq 1$, but may approach the limit of $R \to 1$.

Working this through, it is found that

$$Q_{L,back}/L_{ed} = \tfrac{2}{3}[\varepsilon_L/(1 - \varepsilon_L)](H_{L,cz} - H_L) \times \sqrt{[2g(H_{L,cz} - H_L)]} \quad (7)$$

which can be made dimensionless as

$$[Q_{L,back}/(L_{ed}H_{L,cz})]/\sqrt{(gH_{L,cz})} = (8/9)^{1/2}[\varepsilon_L/(1 - \varepsilon_L)][1 - (H_L/H_{L,cz})]^{3/2} \quad (8)$$

For the condition that the total forward flow has to be equal to $RQ_{L,back}$, the equation $R(1 - H_L/H_{L,cz})^{3/2} = 2(H_L/H_{L,cz} - \varepsilon_L)^{3/2}$ has to be fulfilled. A simple linear relation between the liquid height ratio and liquid volume fraction, with coefficients depending on R, was found to do this

$$H_L/H_{L,cz} = [R^{2/3}/(R^{2/3} + 2^{2/3})] + [2^{2/3}/(R^{2/3} + 2^{2/3})]\varepsilon_L \quad (9)$$

Again using the assumption of linearity of the liquid height profile in the contacting area, the liquid height above the level of the weir can be found by: $H_{ow,ca} = H_L(H_B - H_w)/H_B$. Next, substitute the above Eq. (9) for the liquid height ratio, as well as the relation of the liquid height on the calming zone $H_{L,cz} = H_w + H_{ow,Fr}$. Then it is found that the 'weir crest' in the contacting area depends on the parameters ε_L, R, H_w and the clear liquid Francis' weir crest, $H_{ow,Fr}$

$$H_{ow,ca} = \{[R^{2/3}/(R^{2/3} + 2^{2/3})] + [2^{2/3}/(R^{2/3} + 2^{2/3})]\varepsilon_L\} \times (H_w + H_{ow,Fr}) - \varepsilon_L H_w \quad (10)$$

Rewritten as a ratio of weir crest values, this ratio depends on ε_L, R and the ratio $H_{ow,Fr}/H_w$

$$H_{ow,ca}/H_{ow,Fr} = (1 + H_w/H_{ow,Fr})\{[R^{2/3}/(R^{2/3} + 2^{2/3})] + [2^{2/3}/(R^{2/3} + 2^{2/3})]\varepsilon_L\} - \varepsilon_L H_w/H_{ow,Fr} \quad (11)$$

Admittedly, the presented 'edge-vortex' model is rudimentary, as it was developed primarily to test its suitability. Having shown its value, it can be developed further, for instance by including the non-uniform distribution of the liquid volume fraction along the height of the dispersion. However, in order to do this, a model will be needed for the average porosity and the porosity profile in the contacting area, which is beyond the scope of this paper. A logical step forward would be the synthesis of a more comprehensive model of the tray hydraulics by integrating the 'edge-vortex' model and the stochastic flow model.

6. Interpretation of weir crest data

6.1. No calming zone: 'splashing of drops' model

The three sieve tray data sets of Pinczewski, Hofhuis/Meijer and Wijn/Peer (no calming zone) line up well in Fig. 3. The measured values are consistently below those predicted by Francis' equation (for clear liquid) and show some scatter, at least partly resulting from experimental error. The two data sets which show large deviations are the set with a long calming zone of Wijn/Peer and the Hofhuis/van Driesten data, which were obtained with a calming zone of intermediate length. These exceptions will be discussed below (Section 6.2). The results suggest that the influence of the plate geometry (hole diameter, hole pitch and free area) does not extend into the upper spray layer. It is as if the influence of the holes has been scrambled by a randomizing mechanism in the intervening layer.

This was further explored for a valve tray layout. In Fig. 5 the valve tray weir crests are compared with the weir crest from Francis' equation (for clear liquid). The measured values are again below the predicted values. The result is similar to the results for sieve trays (with no or a short L_{cz}). The lack of an effect of the ten-fold variation in gas flow rate is important. On the tray, a spray layer sits on top of a liquid-continuous heterogeneous bubbling layer directly over the valves. From the shape of the density profiles, the transition of spray to heterogeneous layer can usually be identified and its position located. Mostly, the top of this heterogeneous layer is below the weir level and only droplets splash over the weir (open triangles in Fig. 5: $H_o \geq H_w$). However, at the highest weir loads, the heterogeneous layer extends above the weir and flows over, together with the upper spray layer (filled triangles: $H_o \geq H_w$). For these conditions, the weir crest expected on the basis of Francis' equation is approached more closely.

Most of the weir crest data for sieve and valve trays presented here (except a part of the valve tray data) were obtained for operation in a two-layered flow regime: an upper layer of spray with a liquid continuous heterogeneous bubbling layer underneath. In this regime the Francis' weir flow equation overpredicted the experimental weir crest. The linear weir crest equation of the stochastic flow model successfully correlated the weir crest data for both sieve trays and valve trays up to specific weir loads of $Q_L/L_w < \cong 4 \times 10^{-3}\ m^3\ s^{-1}\ m^{-1}$. Surprisingly, the average droplet flow velocity derived from the model was found to be rather constant. Although an effect of gas flow rate, hole size, hole pitch and free area could not be established, an effect of tray type on the weir flow velocity was noticed. For sieve trays, it was $u_{L,ow} = 0.31 \pm 0.06\ ms^{-1}$ and for the valve tray it was $u_{L,ow} = 0.51 \pm 0.10\ ms^{-1}$. These simple rules reflect the current status of development of this subject. When more data of better accuracy become available, the situation will undoubtedly be shown to be more complex. Already, deviation from the simple behaviour can be seen at the extremes of the weir load range. At low specific weir loads, deviations are encountered when the intervening layer breaks down and a low density spray layer forms directly above the holes or valves. When this happens, droplet break up and projection become directly controlled by the high velocities downstream of the holes or the valves in the tray floor. At high specific weir loads, deviations occur because of the influence of a net forward liquid flow velocity in the contacting area, which can no longer be neglected, and a Francis' weir flow contribution by the (aerated) liquid-continuous layer, when this underlying layer rises above the outlet weir.

The results obtained so far can be rationalized as follows. Droplets ejected into the upper gas-continuous spray layer 'inherit' their movements from the lower liquid-continuous layer. The random motions in this heterogeneous bubbling layer derive their kinetic energy from the gas which is injected via the holes in the tray deck. The randomizing motions in the intervening layer remove any influence of the length and time scales associated with bubbling or jetting at the holes. However, an effect of the difference in radial outflow characteristics (and associated difference in gas pressure drop coefficient) between sieve and valve trays can still be noticed in the motions of droplets in the upper spray layer and hence in the weir flow rate.

It is of interest to compare the *horizontal* droplet velocity with the *vertical* droplet projection velocity. In order to do this for sieve trays, use is made of Stichlmair's relation. For the range of gas velocities (load factors) covered $0.03 < \lambda_{ca} < 0.10\ ms^{-1}$, the range of expected vertical droplet projection velocities varies as $0.3 < U_o < 1.0\ ms^{-1}$. Consequently, the velocity ratio drops from $u_{L,ow}/U_o \cong 1$ at low load factors to $u_{L,ow}/U_o \cong 0.3$ at high load factors. So, the ratio shows a decrease in variability (disorder) with increasing gas flow rate. As the weir flow velocity is a measure for the spread in horizontal liquid phase velocities in the contacting area, this result confirms that the behaviour of the two-phase layer is highly dynamic and characterised by large velocity variations.

6.2. With long calming zone: the 'edge-vortex' model

The 'edge-vortex' model leads to a specific relation between the liquid heights on the calming zone and the

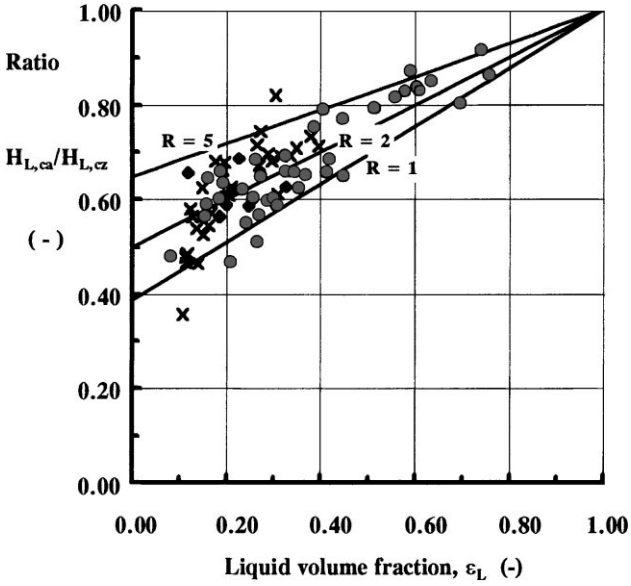

Fig. 8. Liquid height ratio.

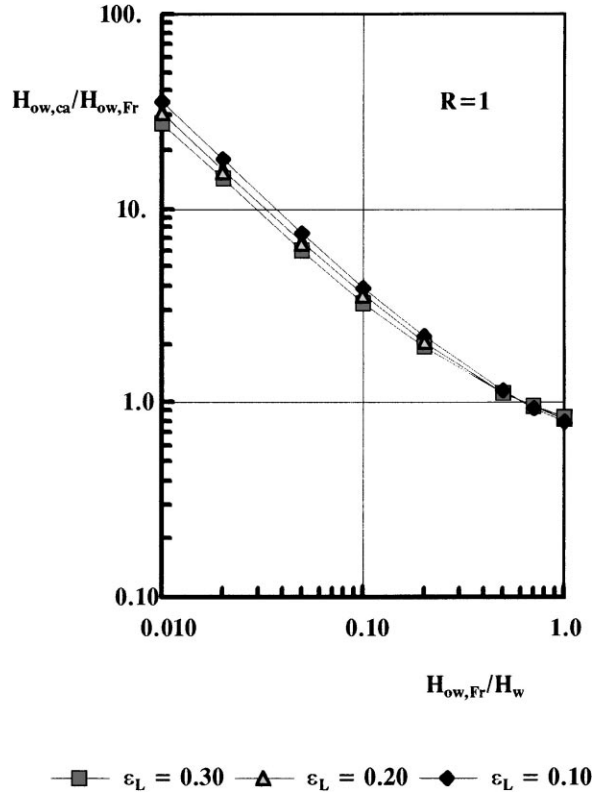

Fig. 9. Weir crest ratio: $H_{ow,ca}/H_{ow,Fr}$.

contacting area, as given by Eq. (9). In Fig. 8, this equation is compared with available experimental data for the sieve trays of Hofhuis/van Driesten (◆) and Wijn/Peer (×) and for the valve tray of Wijn/Konijn (●). The three curves were derived for the values: $R = 1$, 2 and 5. The equation correctly predicts the liquid height ratio to have a value of less than unity. Also, the effect of the liquid volume fraction of the dispersion in the contacting area is described properly. In the experiments, the ratio R was not measured, but as there is a net outflow $R \geq 1$ and the experimental data points lie on or above the line for $R = 1$, as they should. Considering the limited accuracy of the experimental liquid height ratio, the agreement is quite good.

Fig. 9 shows the behaviour of Eq. (11) for $R = 1$ and at specified values of the liquid volume fraction. The figure demonstrates that the weir crest ratio is expected to differ significantly from the value of unity (corresponding to Francis' weir flow case). In the 'edge-vortex' model, this stems from the liquid recycle, which increases the liquid volume fraction and expands the gas–liquid dispersion in the contacting area where the weir crest contribution is measured. Clearly this weir crest cannot be the same as for clear liquid flow over the weir, as in Francis' weir flow. In this paper, only a small sample of Zuiderweg and Hofhuis' data has been used. An overview of *all* their weir crest data can be inspected in Zuiderweg et al. [Fig. 2 in [15]]. These authors used a different group of variables to correlate their weir crest ratios empirically. Their correlating group was defined as flow parameter (FP) divided by specific weir length (b) FP/b, which is equivalent to $(Q_L/L_w)/\lambda$. Also, observing that the weir crest H_{ow} increases with increasing weir load (Q_L/L_w) and that the liquid volume fraction decreases with increasing gas load factor λ, their correlation can readily be reconciled with the presented edge-vortex model. The severe deviations from Francis' weir flow shown in their test data could have been expected for a tray with a long calming zone. This shows that the assumption of 'an equal weir crest H_{ow} at the weir and in the contacting area' is untenable.

The long calming zone tests of Wijn/Peer can now be interpreted with the 'edge-vortex' model in two ways by estimating: the liquid flow rate in the vortex and the 'weir crest' contribution to the liquid height in the contacting area. Firstly, Eq. (7) has been used to estimate the backflow rate $Q_{L,back}/L_{ed}$ through the 'dynamic and open weir' at the edge. With $0.1 < \varepsilon_L < 0.3$, $0.5 < H_L/H_{L,cz} < 0.7$ and $0.04 < H_{L,cz} < 0.07$ m, the range of expected values is calculated to be $\approx 6 \times 10^{-4} < Q_{L,back}/L_{ed} < \approx 7 \times 10^{-3}$ m^3 s^{-1} m^{-1}. These calculated vortex flow rates are an order of magnitude higher than the experimentally measured forward flow rates. So the value of R is only a little above unity. Basing the vortex flow rate on the backflow rate and neglecting the net forward flow was justified after all. Replotting in Fig. 3 the measured weir crests on the basis of the calculated 'open weir' flow rates would shift them in line with the other sieve tray data. This being the case, it should be allowable to use the weir crest relation of the stochastic spray model in reverse to estimate specific flow rates from the measured weir crests. In this way, the range of expected values is found to be $\approx 1 \times 10^{-3} < Q_{L,back}/L_{ed} < \approx 3 \times 10^{-2}$ m^3 s^{-1} m^{-1}. As this range largely overlaps the range estimated by the 'edge-vortex' model, it confirmed the large

increase in liquid flow rates. The significance of this is also that the liquid flow over the boundary of the contacting area and calming zone is governed by the same stochastic flow mechanism operating at an outlet weir without a calming zone. Secondly, Eq. (10) can be used to estimate the 'weir crest' contribution to the liquid height in the contacting area. For $\varepsilon_L = 0.1$, the expected $H_{ow,ca}$ values vary between 0.035 and 0.040 m. For $\varepsilon_L = 0.3$, the expected $H_{ow,ca}$ values vary between 0.027 and 0.033 m, for the entire range of experimentally measured weir flow rates. These calculated 'weir crest' values are about 20 times larger than those based on Francis' weir equation. Also, they are about twice as large as the measured 'weir crest' values. This was expected, as the assumption of a constant ε_L independent of height overestimates the local ε_L in the top of the dispersion and underestimates the local ε_L in the bottom of the dispersion. Overall, the simple 'edge-vortex' model gives a satisfactory explanation of the large increase in the experimental 'weir crest' in the presence of a long calming zone, by a large increase in the liquid flow rate passing through the upper part of the two-phase layer and the distribution (expansion) of this recycling liquid over a large height.

In summary, two relations for calculating the liquid height in the contacting area were obtained. The first in the absence of a calming zone and operation in the spray regime

$$H_L = \varepsilon_L H_w + 2(Q_L/L_w)/u_{L,ow}$$

and the second for a long calming zone and with clear liquid exiting over the weir

$$H_L = \{[R^{2/3}/(R^{2/3} + 2^{2/3})] + [2^{2/3}/(R^{2/3} + 2^{2/3})]\varepsilon_L\} \times (H_w + H_{ow,Fr}).$$

Casting these equations in the form $H_L = \alpha H_w + \gamma Q_L/L_w$, using typical values for H_w and $Q_L/_{Lw}$ and linearizing the Q_L/L_w-term (at $Q_L/L_w = 0.01\ m^3\ s^{-1}\ m^{-1}$) yields the following ranges for the experimental coefficients α and γ. In the absence of a calming zone and operation in the spray regime $\alpha \approx 0.1$–0.3 and $\gamma \approx 4$–7. For a long calming zone and with clear liquid exiting over the weir $\alpha \approx 0.5$–0.8 and $\gamma \approx 1.5$–2.4.

These coefficients can be used to gauge the results of earlier investigations, as done in the next section. The first relation sets a lower boundary and the second one an upper boundary on the liquid height. Note the opposing behaviour of the coefficients α and γ with an increasing length of the calming zone. This behaviour complicates the proper interpretation of tests done with intermediate calming zone lengths [21].

7. Old liquid height relations

From the results of the early method of correlating the liquid height (addition of linear terms), one can directly evaluate the influence of the specific weir load, Q_L/L_w. This method works most accurately for large values of Q_L/L_w, where the H_{ow}-contribution is largest. For sieve trays (Table 2) and valve trays (Table 3), results for liquid height correlations obtained from the literature are reviewed below. The tables are a modification and extension of those presented by Lockett (Tables 3.3 and 3.4 in Ref. [22]). Some material was added as a result of correlation of the data in several references [31–33] by the present author.

The constants in the last three rows of Table 2 were obtained by the present author by regression of the data of Weisshuhn [32], van Driesten [33], Porter et al. [34]. These reproduce their experimental liquid heights within 3–4 mm liquid for the liquid height $20 < H_L < 60$ mm. In half of the references, the length of the calming zone is not available. Thomas et al. [28,30,31] produced a large amount of information for sieve trays with long calming zones. So did Brambilla et al. [29]. The liquid heights given by Brambilla et al. are higher than those of the other correlations. A possible reason is that their liquid height measurements were affected by two edge-vortices, one at the tray inlet and the other at the outlet. These edge vortices extended onto the perforated area. The horizontal scale of the edge vortices may well have been larger than the length of the perforated area (0.15 m), increasing the liquid height on the contacting area to the value for the calming zone. Either a long perforated area should be used to properly measure liquid heights in the centre of the contacting area or the calming zones should be replaced by a perforated area.

The tables show that: increasing the weir height increases the liquid height $0.19 < \alpha < 0.49$; increasing the gas flow decreases the liquid height $-0.014 < \beta < 0$; increasing the liquid flow increases the liquid height $1.0 < \gamma < 4.5$; and we need a constant to obtain a good correlation; this constant δ may be related to the minimum liquid height required to operate a tray.

The range of values for the weir height coefficient α and the weir load coefficient γ compare well with the values expected on the basis of the equations presented above; these 'embrace' the entire range of values of the old liquid height relations. The implication is that differences in the length of the calming zone can explain the variation in the reported weir height and weir flow coefficients.

Apart from the effect of the calming zone, the surface properties of the test systems are also important. An example from the work of Thomas and collaborators demonstrates this. Changing the test system from an aqueous 1 N sodium carbonate solution to an aqueous glycerol solution made it more viscous and more foamy. This affected the γ values reported, which can be interpreted as a reduction in weir flow velocity from $u_{L,ow}$ $(=2/\gamma) = 0.9\ ms^{-1}$ to $u_{L,ow} = 0.5\ ms^{-1}$. This can be explained by a reduction in the rate of bubble coalescence. In the carbonate solution, larger bubbles ('voids') may be formed than in the glycerol solution, thus leading to larger liquid displacement velocities. The study of Finch and van Winkle [26] reported the

Table 2
Empirical liquid height relations for sieve trays

Sieve trays	$H_L = \alpha H_w + \beta F + \gamma(Q_L/L_w) + \delta$ (SI units)								
Reference	α	β	γ	δ	D_h (mm)	f_h (%)	H_w (mm)	L_{cz} (mm)	System
[23]	0.372	−0.014	1.78	0.024	4.8	5.7	50; 75; 100	n.a.	air–water
[24]	0.580	$-0.017H_W$	3.68	0.006	4.8			n.a.	air–water
[25]	0.725	$-0.022H_W$	1.02	0.006	4.8	4.2; 8.2; 11.3		n.a.	air–water
[26]	0.220	−0.012	4.54	0.025	1.6–8			n.a.	air–water/methanol
[27]	0.190	−0.014	2.04	0.042				n.a.	
[28]	0.190	−0.008	1.32	0.040	3.2	10.1	75; 100	152	air/aq. glycerol (55% water)
[29]	0.770	−0.028	2.66	0.005	3.0	10.0	30; 40; 50; 60; 70	?100–150?	air–water
[29]	0.790	−0.028	2.52	0.005	4.0	12.0	30;40; 50; 60; 70	?100–150?	air–water
[29]	0.720	−0.028	2.16	0.003	5.0	10.0	30; 40; 50; 60; 70	?100–150?	air–water
[30]	0.490	−0.003	2.21	0.039	9.5	10.8	75; 100	152	1 N Na_2CO_3
[30]	0.420	−0.003	3.93	0.031	9.5	10.8	75; 100	152	air/aq. glycerol (50% water)
[31]		−0.003	3.27	0.056	9.5	12.4	75	194	air–water
[31]		−0.003	1.84	0.069	25.4	12.4	75	194	air–water
[31]		−0.004	2.04	0.056	25.4	11.8	75	142	air–water
[32]	0.235	−0.002	2.00	0.005	2.5	3; 9; 12	30; 50; 75; 100	n.a.	air/(hot)water
[33]	0.320	−0.002	1.20	0.012	7.0	10.0	25; 50	100	air–water
[34]	0.350	0.000	2.00	0.013	6.4	10.0	10; 20; 50	n.a.	air/(hot)water
Minimum:	0.190	−0.028	1.02						
Maximum:	0.790	0.000	4.54						
Average:	0.462	−0.012	2.50						
Standard deviation:	0.247	0.010	1.01						

highest γ value in the whole sieve tray set. They used the air–water–methanol system, which is known to display coalescence inhibiting characteristics.

A transition in flow regime can also complicate the proper interpretation of old data. The result from correlating the liquid height data for a Glitsch V1 valve tray, as reported by Dhulesia [35], gave the weir flow velocity $u_{L,ow} = 2.0\ ms^{-1}$. This finding is in support of the higher weir flow velocities on valve trays than on the sieve trays. For the Shell/Metawa valve tray reported above, the result was $u_{L,ow} = 0.5\ ms^{-1}$. The higher velocity on the Glitsch V1 tray is probably related to the greater size and weight of the valves used. This has contributed to the establishment of a low liquid height on the tray. This favours the development of a situation in which a 'fully developed' spray layer sits directly on top of the valves, without an intervening heterogeneous layer. On the valve tray with Shell/Metawa valves, this situation was achieved only at the lowest weir flow rates applied. Then the weir crests were also reduced. Note, that such high liquid weir flow velocities (low γ values) have been seen in a number of sieve tray correlations (see Table 2). These may have to be attributed to operation in this 'fully developed' spray flow regime. More work is needed to confirm this.

8. Examples of applications

The new insights help us to understand the effect of modifications to a tray at its outlet (Fig. 10).

The use of a vertical baffle directly in front of an outlet weir, a so-called '*splash*' *baffle*, is mentioned by Jones and Pyle [36]. It was introduced to make the two-phase behaviour on sieve trays look more like that on bubble cap trays. It helped control what was called the 'splashing' or 'geysering' action. It also increased the liquid height on the tray. The 'splash baffle' intercepts droplets being ejected over a weir. The increase in liquid height helps to improve the tray efficiency [37], but reduces both the maximum and minimum capacity. Nowadays, splash baffles are seldom used.

A vertical '*anti-jump*' *baffle* is often placed in the centre of downcomers of multi-pass or multi-downcomer trays.

Table 3
Empirical liquid height relations for valve trays

Valve trays	$H_L = \alpha H_w + \beta F + \gamma(Q_L/L_w) + \delta$ (SI units)								
Reference	α	β	γ	δ	D_h (mm)	f_h (%)	H_w (mm)	L_{cz} (mm)	System
[29]	0.740	−0.014	1.66	0.0150–0.045	21–26		30; 40; 50; 60; 70	?100–150?	air–water
[35]	0.70–0.15F	0.000	0.97	0.0	38		25; 50; 75	50	air–water

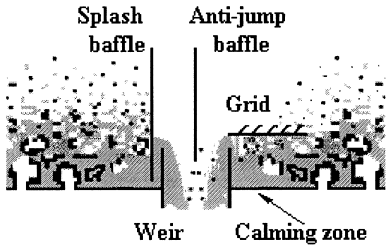

Fig. 10. Tray outlet auxiliaries.

The Glitsch Design Manual [38] contains an example. A Shell paper [39] shows them mounted in the downcomers ('calming sections') of their multi-downcomer trays. UOP applies them in their MD-trays [40]. Droplets ejected from the tray can jump over the entire downcomer. Above the jumping distance has been estimated as $L_{50\%} \cong 0.67\ \lambda_{ca}$. For typical operating conditions, this leads to jump distances of 5–10 cm. So, for narrow downcomers, a vertical anti-jump baffle intercepts part of the splashing and increases the downcomer capacity, and thus is of direct commercial benefit.

Instead of a vertical and closed baffle, a grid or expanded metal sheet (or any other horizontal, high open area sheet metal) can be placed over the outlet weir. This sheet intercepts drops and reflects them down again. A clearance left open between the edge of the open 'sheet' and the weir allows liquid to pass through into the downcomer. Former Shell colleagues [41,42] have developed a tray with an expanded metal sheet extending over the entire contacting area. This improved liquid height, downcomer capacity and, at the same time, reduced entrainment, thus giving lower product contamination.

9. Conclusions

On a distillation tray, the liquid height is determined by the way liquid flows over the outlet weir into the downcomer. This does not occur in the same way as for the flow of a clear liquid, but by a splashing mechanism. Because of this, a non-gassed zone (calming zone) next to the downcomer has a large effect. At the edge of the gassed zone (the contacting area) on a tray, the splashing mechanism controls the liquid flow. On one side of the edge, in the gassed zone, the liquid is expanded, atomized and lifted. On the other side, in the calming zone, the drops fall out. A pressure gradient causes the liquid to return to the gassed zone and an edge-vortex is set in motion. Modelling the liquid flow for such an edge-vortex gives a correct description of the weir crest contribution to the liquid height. For trays with a long calming zone, Francis' weir crest equation should not be used directly in estimations of the liquid height in the contacting area, as it strongly underestimates the weir crest contribution. A new equation is proposed, which includes Francis' contribution in the proper way. For trays without a calming zone, the contacting area extends right up to the weir, the edge-vortex can be neglected and the splashing rate of droplets directly controls the weir flow rate. The concepts developed and insights gained in this work help us to understand the effects of certain hardware changes near the outlet end of a tray. Steps can now be taken to develop more realistic hydraulic models for trays.

Acknowledgements

The author is grateful to Shell International Oil Products B.V. for their continued support and for allowance to make use of the experimental data generated during his employment at Shell Research and Technology Centre, Amsterdam. The contributions of A. (Andre) Peer and G. (Gert) Konijn were indispensable in obtaining these data. Discussions with J. (Hans) A. Wesselingh have been most helpful to the author in clarifying and structuring his thoughts and making him proceed further into uncharted territory.

Appendix

Nomenclature

A_{BA}	'bubbling' area of a tray ($=A_{ca}$)	(m^2)
A_{ca}	contacting area of a tray	(m^2)
A_{col}	cross section of the column	(m^2)
A_h	hole area	(m^2)
d_h	orifice or hole diameter	(m)
f_h	fraction of hole area in contacting area (or basic free area)	
F	F factor, $F = U_g\sqrt{\rho_g} \vee F = \lambda(\rho_L - \rho_g)$	($ms^{-1}\sqrt{(kgm^{-3})}$)
g	gravitational acceleration	(ms^{-2})
H_B	height of two-phase layer (bed height)	(m)
H_{co}	height at which pressure gradients cross over	(m)
H_L	equivalent clear liquid height in the two-phase layer	(m)
$H_{L,ca}$	liquid height in the contacting area	(m)

$H_{L,cz}$	liquid height in the calming zone	(m)
$h_{L,spray}$	equivalent clear liquid height in the droplet layer	(m)
H_o	height of phase transition from liquid- to gas-continuous	(m)
H_{ow}	liquid height over outlet weir	(m)
$H_{ow,ca}$	liquid height over weir level, in the contacting area	(m)
H_w	outlet weir height	(m)
L_{ed}	length of boundary edge ($\cong L_w$)	(m)
L_{cz}	length of unperforated calming zone upstream of outlet weir	(m)
L_{hor}	horizontal travel distance	(m)
L_w	overflow length of outlet weir	(m)
p_h	hole pitch (or distance between holes)	(m)
Q_g	volumetric gas flow rate	($m^3\ s^{-1}$)
Q_L	volumetric liquid flow rate	($m^3\ s^{-1}$)
$Q_{L,back}$	volumetric back flow rate of liquid	($m^3\ s^{-1}\ m^{-1}$)
Q_L/L_w	specific liquid weir load	($m^3\ s^{-1}\ m^{-1}$)
R	ratio of forward over backward flow of liquid	
S_U	variance in horizontal liquid velocity	(ms^{-1})
t	time	(s)
$u_{L,ca}$	horizontal liquid flow velocity, in the contacting area	(ms^{-1})
$u_{L,hor}$	horizontal liquid flow velocity	(ms^{-1})
$u_{L,ow}$	horizontal liquid flow velocity, over weir	(ms^{-1})
U_L	liquid velocity	(ms^{-1})
U_g	gas velocity, based on contacting area	(ms^{-1})
U_b	bubble rise velocity	(ms^{-1})
U_o	initial droplet projection velocity	(ms^{-1})
W_{ca}	width of containing area	(m)

Greek letters

α, β, γ, δ	coefficients	
ε_L	liquid volume fraction in two-phase layer	
$\varepsilon_{L,ow}$	liquid volume fraction, over weir	
$\varepsilon_{L,uw}$	liquid volume fraction, under weir	
λ	load factor $\left(\lambda = F/\sqrt{(\rho_L - \rho_g)}\right)$	(ms^{-1})
λ_{ca}	load factor, based on contacting area	(ms^{-1})
λ_h	hole load factor $[= \left(Q_g/A_h\right)\sqrt{(\rho_g/(\rho_L - \rho_g))}]$	(ms^{-1})
ρ_g	gas density	(kgm^{-3})
ρ_L	liquid density	(kgm^{-3})

Subscripts

b	bubble
ba	'bubbling' area (= contacting area)
ca	contacting area
col	column
df	dense phase
exp	experimental
Fr	Francis
g	gas
h	hole
hor	horizontal
L	liquid
ow	over the weir
uw	under the weir
w	weir

References

[1] P.A.M. Hofhuis, F.J. Zuiderweg, Sieve plates: dispersion density and flow regimes, I. Chem. E. Symposium Series No. 56 (1979) 2.2/1–2.2/26.

[2] D.L. Bennett, R. Agrawal, P.J. Cook, New pressure drop correlation for sieve tray distillation columns, AIChE J. 37 (1983) 589.

[3] C.J. Colwell, Clear liquid height and froth density on sieve trays, Ind. Eng. Chem. Process Des. Dev. 20 (1981) 298–307.

[4] G.P. Solomakha, G.G. Shaubert, V.I. Vashchuk, Calculation of the height of a static liquid layer in plate devices equipped with overflows, Theor. Found. Chem. Eng. USSR 17(6) (1983) 516–525.

[5] L.S. Pozin, G.P. Solomakha, O.L. Shubina, Description of principles determining the level of light liquid on overflow plates, Theor. Found. Chem. Eng. USSR 19(4) (1985) 329–333.

[6] J. Stichlmair, Grundlagen der Dimensionierung des Gas/Flssigkeit-Kontaktapparates Bodenkolonne, Reprotext, Verlag Chemie, Weinheim, 1978.

[7] S. Aiba, T. Yamada, Studies on entrainment, AIChE J. 5(4) (1959) 506–509.

[8] W.V. Pinczewski, C.J.D. Fell, Droplet projection velocities for use in sieve tray spray models, Can. J. Chem. Eng. 49 (1971) 548–549.

[9] D.L. Bennett, H.J. Grimm, Eddy diffusivity for distillation sieve trays, AIChE J. 37(4) (1991) 589–596.

[10] M.J. Ashley, G.G. Haselden, Effectiveness of vapour-liquid contacting on a sieve plate, Trans. Inst. Chem. Eng. 50 (1972) 119–124.

[11] J.A. Raper, M.S. Kearney, J.M. Burgess, C.J.D. Fell, The structure of industrial sieve tray froths, Chem. Eng. Sci. 37(4) (1982) 501–506.

[12] J. Ellenberger, Analogies in multiphase reactor hydrodynamics, Thesis, University of Amsterdam, 1995.

[13] J.W.A. de Swart, Scale-up of a Fischer–Tropsch slurry reactor, Thesis, University of Amsterdam, 1996.

[14] P.A.M. Hofhuis, Flow regimes on sieve trays for gas/liquid contacting, Thesis, Technical University Delft, 1980.

[15] F.J. Zuiderweg, P.A.M. Hofhuis, J. Kuzniar, Flow regimes on sieve trays: the significance of the emulsion flow regime, Chem. Eng. Res. Des. 62 (1984) 39–47.

[16] W.V. Pinczewski, C.J.D. Fell, Nature of the two-phase dispersion on sieve plates operating in the spray regime, Trans. Inst. Chem. Eng. 52 (1974) 294–299.

[17] E.F. Wijn, On the lower operating range of sieve and valve trays, Chem. Eng. J. 70 (1998) 143–155.

[18] C.J. Huang, J.R. Hodson, Perforated Trays, Petroleum Refiner 37(2) (1958) 104–118.

[19] R.F. Detman, How Weir location affects sieve tray pressure drop, Hydrocarbon Processing and Petroleum Refiner 42(8) (1963) 147–151.

[20] A.G. Vikhman, M.A. Berkovski, S.A. Kruglov, Investigating the effect on downcomer width in crossflow mass-transfer tray operation, Chem. Petroleum Eng. USSR 12 (1976) 232–234.

[21] M.J. Lockett, The froth to spray transition on sieve trays, Trans. Inst. Chem. Eng. 59 (1981) 26–34.

[22] M.J. Lockett, Distillation Tray Fundamentals, Cambridge University Press, Cambridge, 1986.

[23] P.R. Barker, M.F. Self, The evaluation of liquid mixing effects on a sieve plate using unsteady and steady state tracer techniques, Chem. Eng. Sci. 17 (1962) 541–553.

[24] I.J. Harris, G.H. Roper, Performance characteristics of a 12 in diameter sieve plate, Can. J. Chem. Eng. 40(6) (1962) 245.

[25] J.A. Gerster, Tray Efficiencies... is more research needed?, Chem. Eng. Prog. 59(3) (1963) 35–46.

[26] R.N. Finch, M.v. Winkle, A statistical correlation of the efficiency of perforated trays, Ind. Eng. Chem. Proc. Des. Dev. 3(2) (1964) 107–116.

[27] G.A. Hughmark, Point efficiencies for tray distillations, Chem. Eng. Progress 61(7) (1965) 97–100.

[28] W.J. Thomas, M. Campbell, Hydraulic studies in a sieve plate downcomer system, Trans. Inst. Chem. Engrs, 45 (1967) T53–T63.

[29] A. Brambilla, G. Nardini, G.F. Nencetti, S. Zanelli, Hydrodynamic behaviour of distillation columns: pressure drop in plate distillation columns, I. Chem. E., Proc. of the International Symp. on Distillation, Brighton, 1969, pp. 2:63–2:71.

[30] W.J. Thomas, M.A. Haq, Studies of the performance of a sieve tray with 3/8-in. diameter perforations, Ind. Eng. Chem. Proc. Des. Dev. 15(4) (1976) 509–518.

[31] W.J. Thomas, O. Ogboja, Hydraulic studies in sieve tray columns, Ind. Eng. Chem. Proc. Des. Dev. 17(4) (1978) 429–443.

[32] E. Weisshuhn, Untersuchungen zum Bodenverstrkungsverhltnis unter Bercksichtigung der Flssigkeitsvermischung in der Sprudelschicht, Chem.-Ing.-Techn. 48 (1976) 3, MS 333/76.

[33] P. van Driesten, Het Porositeits Profiel: Middel tot Beschrijving van Twee-fasen Mengsels op Zeefplaten, Verslag 5e jaars onderzoek, TH Delft, 1977.

[34] K.E. Porter, K.T. Yu, S. Chambers, M.Q. Zhang, Flow patterns and temperature profiles on a 2.4 m. diameter sieve tray, I. Chem. E. Symp. Series 128 (1992) A257–A272.

[35] H. Dhulesia, Clear liquid height on sieve and valve trays, Chem. Eng. Res. Dev. 62 (1984) 321–326.

[36] J.B. Jones, C. Pyle, Relative performance of sieve and bubble-cap plates, Chem. Eng. Prog. 51(9) (1955) 424–428.

[37] E.F. Wijn, Does the point efficiency on sieve trays depend on liquid height and flow regime?, I. Chem. E. Symp. Series 142(2) (1997) 809–816.

[38] Glitsch, Inc., Ballast Tray Design Manual, Bulletin No.4900 (Revised), 1961.

[39] F.J. Zuiderweg, J.H. de Groot, B. Meeboer, D. van der Meer, Scaling up distillation plates, I. Chem. E., Proc. of the International Symp. on Distillation, Brighton, 1969, pp. 5:78–5:83.

[40] M.R. Resetarits, M.J. Lockett, UOP, Multiple-downcomer fractionation tray with vapour directing slots and extended downcomer baffles, Patent No. US 5,382,390, 1995.

[41] W.H. Smit, H.J. Scheffer, J.H. de Groot, A gas–liquid contact tray, Patent No. GB 1250703, 1971.

[42] A.D. Barber, R.C. Darton, The use of expanded metal to improve the operation of sieve trays for vacuum distillation, I. Chem. E., 4th Annual Research Meeting, Swansea, 1977.